

# Design of a Vacuum Pumping System for the Closed Helical Divertor for Steady State Operation in LHD<sup>\*)</sup>

Mamoru SHOJI, Suguru MASUZAKI, Tomohiro MORISAKI, Masahiro KOBAYASHI, Masayuki TOKITANI and Yasuhiko TAKEIRI

*National Institute for Fusion Science, Toki 509-5292, Japan*

(Received 2 December 2011 / Accepted 24 July 2012)

A vacuum pumping system is installed in a Closed Helical Divertor (CHD) in the Large Helical Device (LHD) at the National Institute for Fusion Science for active control of the peripheral plasma density and impurity suppression in the core plasma. In the CHD configuration, the distance between the pumping system and the divertor plates (heat and particle source) is very short (only  $\sim 0.1$  m). One of the major issues in designing the pumping system is the reduction of heat load by radiation and thermal conduction due to the neutral particles being released from the heated divertor plates while keeping a high pumping efficiency. Here the heat load and the pumping efficiency are analyzed using a neutral particle transport simulation and a finite element method based software for multi-physics analysis. We propose a new design for a pumping system with an expanded area of the inlet of the water-cooled blinds and a bottom slit beneath the pumping system. This increases the pumping efficiency by approximately 60% over that of our previous design. It also predicts that the increase in heat load on the pumping system for the new design would be reasonably suppressed by a buffer plate with high emissivity on the surface of the vacuum vessel on the inboard side of the torus.

© 2012 The Japan Society of Plasma Science and Nuclear Fusion Research

Keywords: vacuum pumping system, closed helical divertor, LHD, steady state operation, neutral particle transport simulation, ANSYS, EIRENE, heat load analysis

DOI: 10.1585/pfr.7.2405145

## 1. Introduction

The design of the vacuum pumping system in future fusion reactors requires properties such as helium ash removal, impurity suppression in the core plasma, and neutral particle pumping for active control of the peripheral plasma density. Two test modules for investigating the performance of the closed helical divertor (CHD) were installed in the inboard side of the torus in the Large Helical Device (LHD) in the last experiment campaign (2010y) [1]. The CHD consists of three components: the slanted divertor plates, a dome with slanting sides, and the target plates. It enhances the neutral particle density behind the dome by more than one-order of magnitude compared to that in the original open divertor [2].

In the near future, a vacuum pumping system will be installed behind the dome. Because of the short distance ( $\sim 0.1$  m) between the divertor plates and the pumping system, we need to take into account the heat loads from thermal conduction due to neutral particles and from radiation from the heated divertor plates. Here, we propose a design for the pumping system that is based on analyses of the pumping efficiency and the heat load, which is an improvement over our previously proposed one [3].

## 2. Vacuum Pumping System for Closed Helical Divertor Configuration

The vacuum pumping system is made up of three components: water-cooled (WC) blinds, liquid nitrogen (LN<sub>2</sub>)-cooled chevrons, and a gas/liquid helium (LHe)-cooled panel (see Fig. 2 in Ref. 3). Two mechanisms transfer the heat from the divertor plates to the LHe-cooled panel. One is thermal conduction due to the kinetic energy of neutral particles and the other is radiation. The LN<sub>2</sub>-cooled chevrons are covered with WC blinds for protecting them from the heat loads. The LHe-cooled panel is surrounded by the LN<sub>2</sub>-cooled chevrons.

A previous analysis using a finite element method based software for multi-physics analysis (ANSYS) and neutral particle transport simulation (EIRENE) showed that this geometrical configuration is effective in suppressing the heat load onto the LHe-cooled panel without serious degradation of the pumping efficiency. The first concern for the pumping system is the heat load on the LHe-cooled panel by thermal conduction in the high density plasma discharge operation which requires a particle pumping rate of about  $1 \times 10^4$  A. The second concern is the heat load due to the radiation from the heated divertor plates in the steady state plasma discharge operation with a relatively low particle pumping rate of about  $1 \times 10^3$  A. Our previous analyses showed that the installation of buffer

author's e-mail: shoji.mamoru@LHD.nifs.ac.jp

<sup>\*)</sup> This article is based on the presentation at the 21st International Toki Conference (ITC21).

plates, on which many deep grooves (1.0 mm deep and 0.5 mm wide) are hollowed out, is effective in suppressing the heat load by thermal conduction [3]. In the next section, three different configurations of the pumping system are investigated from two viewpoints: pumping efficiency and heat load by thermal conduction/radiation.

### 3. Analyses of Pumping Efficiency and Heat Load by Thermal Conduction

#### 3.1 Model of a pumping system for neutral particle transport simulation

The pumping efficiency and heat loads were analyzed using the EIRENE [4]. The measured neutral particle pressure behind the dome is in the order of 0.1 Pa (in the molecular flow regime), which ensures that a Monte Carlo based particle tracking approach is appropriate for the analysis of the neutral particle transport [1]. An example of the geometrical model of the CHD configuration and the pumping system for the simulation is shown in Fig. 2 of Ref. 3. The model simulates the configuration of the pumping system installed on the equatorial plane in the torus, which means that the following analyses give the heat loads on the higher side because the distance between the divertor plates and the pumping system is geometrically the shortest one.

Figure 1 gives a cross section of the model which shows small rectangular grids used for calculating the neutral particle density profiles. The model includes the geometrical configuration of the LHD peripheral plasma (divertor leg), which is determined by a magnetic field line traced from the main plasma with a particle diffusion ef-

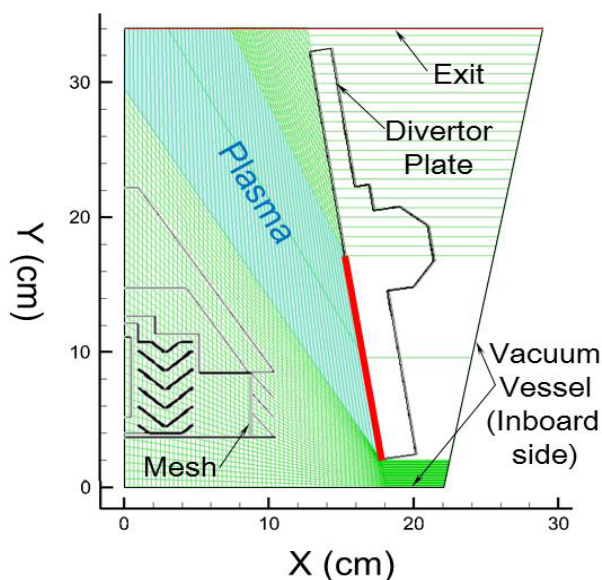


Fig. 1 Cross-section of a model of the pumping system with small rectangular grids for calculating neutral particle density profiles.

fect [2]. The plasma wetted area on the surface of the divertor plate is determined by the distribution of the strike points of the magnetic field lines on the surface. It is assumed that the plasma density and the electron/ion temperature on the divertor leg are fixed at  $1 \times 10^{19} \text{ m}^{-3}$  and 30 eV, respectively, which are typical values in the inboard side of the torus for an inward magnetic axis shift configuration. The profile of the above two plasma parameters on the divertor leg is set as constant because of the short connection length of the magnetic field line on the divertor leg (less than about 3 m).

The pumping efficiency is defined as the ratio of the current of neutral particles reaching the LHe-cooled panel ( $I_{\text{He}}$ ) to the total plasma current flowing to the divertor plates ( $I_{\text{Div}}$ ). The neutral current is obtained by tracking the test particles (representing the neutral hydrogen atoms/molecules) released from the divertor plate in the simulation. The heat load by thermal conduction onto a component in the pumping system is calculated by summing all the deposited kinetic energy of the test particles colliding with the component ( $E_{\text{dep}}$ ). The deposited energy is obtained by the following formula:

$$E_{\text{dep}} = E_{\text{col}} - E_{\text{ref}},$$

where the parameter  $E_{\text{col}}$  is the kinetic energy of the neutral particles colliding with the component, and  $E_{\text{ref}}$  is the energy of the neutral particles reflected from the component. In order to consider the energy interactions between the neutral hydrogen molecules and the component, an accommodation coefficient  $\alpha$  is introduced. When a hydrogen molecule reaches the surface of a component, a normalized uniform random number  $\rho$  is generated. If  $\rho$  is smaller than  $\alpha$ , the energy of the reflected hydrogen molecules is set to the energy corresponding to the temperature of the component. Otherwise, the energy of the reflected molecules is not changed. Following the discussion in Ref. 5, the parameter  $\alpha$  is set to 0.2. When a hydrogen atom reaches a component, the following two processes are selected depending on the particle reflection ratio calculated by the TRIM code. In the first process the atom is reflected from the surface with a kinetic energy determined by the code. In the other, a molecular hydrogen with a reduced statistical weight is released with an energy corresponding to the surface temperature. The physical properties and temperature of the components are the same as those in our previous analyses [3].

#### 3.2 Improvement of pumping system design

To improve the design of the pumping system, the pumping efficiency and the heat loads were calculated for three different geometries. Half profiles of the cross-sections of the pumping system in the three geometries are illustrated in Fig. 2. Type-I is the original configuration previously proposed [3]. Type-II is a configuration with an expanded area of the inlet of the WC blisks with a narrow sized dome structure for efficiently introducing neu-

tral particles into the pump. Type-III has a slit at the bottom plate of the WC components in order to collect neutral particles trapped beneath the pumping system. In all the configurations, the buffer plates are installed on the surface of the WC components and the LN<sub>2</sub>-cooled chevrons. A 50% transparent mesh is inserted into the space between the WC- and LN<sub>2</sub>-cooled components for protecting the LHe-cooled panel from microwave heating.

### 3.3 Calculations of the neutral particle density profile

Figure 3 shows the calculated density profiles of the neutral hydrogen molecules in the three geometries. Note that the neutral density in the space between the WC blinds and the LN<sub>2</sub>-cooled chevrons rises significantly in

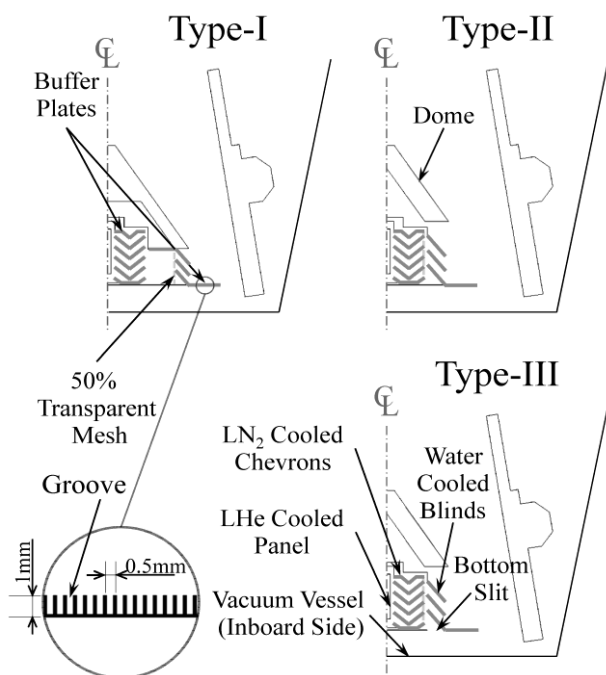


Fig. 2 Cross-section of three different geometries of the pumping system for the CHD.

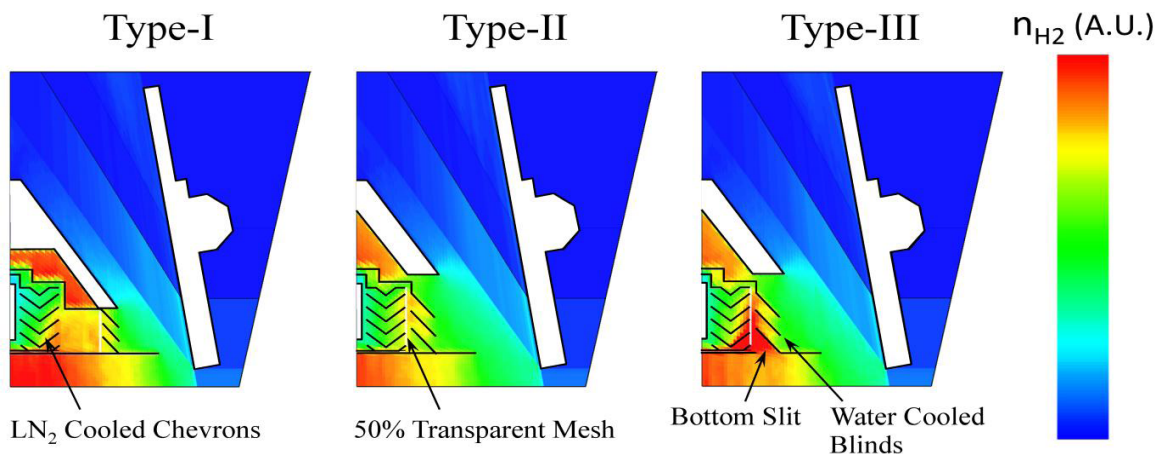


Fig. 3 Calculated density profiles of neutral hydrogen molecules in the three geometries of the pumping system.

the Type-III configuration, which means that the two modifications (the expanded inlet and the bottom slit) increase the amount of neutral particles introduced in the pumping system. The calculated pumping efficiency and the heat load on the three components in the three geometries for  $I_{Div} = 1$  A are shown in Fig. 4. The pumping efficiency is significantly improved by the two modifications; however, the two modifications also increase the heat load on the LN<sub>2</sub>-cooled chevrons. A buffer plate installed on the surface of the vacuum vessel on the inboard side of the torus can suppress the heat load. A simulation that includes the buffer plate on the inboard side shows that the buffer plate reduces the heat load on the chevrons by a factor of approximately four while retaining the pumping efficiency (Fig. 4).

### 3.4 Estimation of the heat loads by thermal conduction on the pumping system

The required particle pumping current in the high

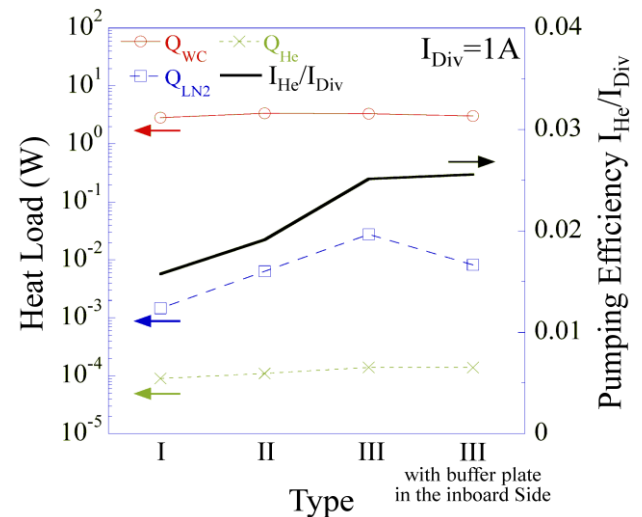


Fig. 4 Calculated pumping efficiency and heat loads by thermal conduction due to neutral particles on the three components of the pumping system.

density plasma discharge operation is about  $10^4$  A. When this is achieved, the heat loads on the three components (WC blinds, LN<sub>2</sub>-cooled chevrons, and LHe-cooled panel) for the full torus geometry in the Type-III configuration (with the buffer plate on the inboard side) are estimated to  $1.2 \times 10^6$ ,  $3.2 \times 10^3$ , and  $8.2 \times 10^1$  W (including the heat of condensation of H<sub>2</sub> on the LHe-cooled panel), respectively.

### 3.5 The effect of the mesh on the pumping efficiency

We investigated the effect of the 50% transparent mesh by comparing the pumping efficiency in the Type-I configuration for the cases with and without the mesh, and found that reduction of the pumping efficiency is about 10%. The reason for the relatively small effect on the pumping efficiency by the mesh is that the escape of neutral particles reflected from the LN<sub>2</sub>-cooled chevrons to the WC blinds is suppressed by the mesh, while the entry of neutral particles to the chevrons is disturbed.

## 4. Analysis of Heat Loads by Radiation

The second concern when designing the pumping system is the heat loads by radiation from the heated divertor plates in the steady state plasma discharge operation. The heat load was calculated using ANSYS with a two-dimensional model and assuming that the temperature on the lower half surface of the divertor plate is 1000°C. This assumption is reasonable because the divertor plasma directly attaches a position on the lower half of the divertor plates, and each plate is composed of two separated carbon plates attached to a water cooled pipe (the heat transmission between the two carbon plates is low). The assumed surface temperature is the allowable upper limit for the steady state operation, which means that the calculated heat loads give the maximum estimations.

The temperature of the water cooled pipes for cooling the divertor plates and the dome is set to 30°C. The physical properties of the components of the pumping system and the vacuum vessel follow those in the previous analysis [3]. The emissivity of the WC/LN<sub>2</sub>-cooled and LHe-cooled components in the pumping system is assumed to 0.9 and 0.2, respectively. And, the emissivity of the surface of the divertor plate and the vacuum vessel is set to 0.8 and 0.2, respectively.

The calculations of the heat loads on the three components in the Type-II and Type-III configurations for the full torus geometry are given in Fig. 5. The heat load on the LN<sub>2</sub>-cooled chevrons rises in the Type-III by a factor of approximately two compared to that in the Type-II, and is caused by the radiation reflected from the surface of the inner vacuum vessel through the bottom slit. The heat load on the chevrons in the Type-III can be reduced by increasing the emissivity on the surface of the vacuum vessel in the inboard side of the torus. The calculated heat loads

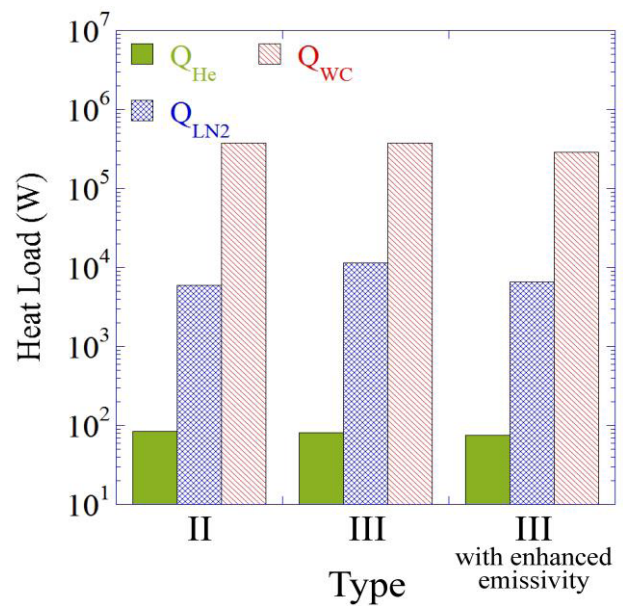


Fig. 5 Calculated heat loads by radiation on the three components of the pumping system.

on the three components with an enhanced emissivity (0.9) on the inner vacuum vessel are also shown in Fig. 5 (the rightmost bars), showing that this modification is effective for controlling the heat load on the chevrons without any serious drawbacks.

The co-deposition layers of metals and carbons accumulated on the surface of the inner vacuum vessel behind the pumping system would play a crucial role in this function [6]. The co-deposition layers could also work as a buffer plate, which effectively contributes to the reduction of the heat load by thermal conduction onto the LN<sub>2</sub>-cooled chevrons.

## 5. Summary

Analyses of the pumping efficiency and heat loads for three designs of the pumping system showed that the Type-III configuration with a buffer plate with an enhanced emissivity on the surface of the inner vacuum vessel is a promising candidate of the pumping system. This configuration has a higher pumping efficiency by about 60% compared to that in the previously proposed one (Type-I). It shows that a buffer plate with an enhanced emissivity on the inner vacuum vessel is effective for reducing the heat load on the LN<sub>2</sub>-cooled chevrons by thermal conduction and radiation. It also predicts that the reduction of the pumping efficiency due to the installation of the 50% transparent mesh is not a serious problem for the pumping system.

- [1] S. Masuzaki *et al.*, *J. Plasma Fusion Res.* **6**, 1202007 (2011).
- [2] S. Masuzaki *et al.*, *Nucl. Fusion* **42**, 750 (2002).
- [3] M. Shoji *et al.*, *J. Plasma Fusion Res.* **6**, 2401035 (2011).
- [4] D. Reiter *et al.*, *Fusion Sci. Technol.* **47**, 172 (2005).
- [5] R.B. Scott, *Cryogenic Engineering* (D. Van Nostrand, Princeton, N.J., 1959) p. 147.
- [6] M. Tokitani *et al.*, *Fusion Sci. Technol.* **58**, 305 (2010).